Proceedings of CONF-CDS 2025 Symposium: Data Visualization Methods for Evaluation
DOI: 10.54254/2755-2721/2025.PO23471

An Unpowered Hip Exoskeleton Towards Walking Performance Enhancement for Stroke Survivors

Matthew Long

Basis International GuangZhou, Guangzhou, China
18344401998@163.com

Abstract: Stroke is one of the leading causes of long-term disability, often resulting in impaired mobility and decreased life quality. This paper presents a novel passive hip exoskeleton system addressing two critical challenges in post-stroke rehabilitation: multi-planar gait assistance and real-time asymmetry quantification. The design features a geometrically optimized dual-plane assistance mechanism generating simultaneous flexion torque and lateral stabilization through spatial spring coupling. Integrated adaptive frequency oscillators enable sub-100ms gait asymmetry detection, providing instant feedback for users.

Keywords: gait analysis, passive exoskeleton, stroke

1. Introduction

Stroke is one of the leading causes of disability worldwide, with more than 110 million people affected and 38% living with lingering symptoms, such as impaired motor control, due to damage to the central nervous system (CNS) [1]. One of the most debilitating consequences of impaired motor control is gait asymmetry, which affects a survivor's ability to walk efficiently, limiting mobility, increasing energy costs, and elevating fall risks. Hence, improving walking performance is considered one of the main needs of stroke patients during rehabilitation [2].

Wearable exoskeletons, particularly passive devices, are becoming a popular strategy in rehabilitation as they offer non-invasive, cost-effective, and accessible solutions [3]. Unlike powered exoskeletons [4,5] which require external power sources, passive exoskeletons rely on mechanical elements (e.g., springs) to assist the target joints. Several studies have demonstrated their benefits in reducing metabolic cost (e.g., 7% reduction during walking [6]), increasing endurance, and improving range of motion. However, existing implementations predominantly target healthy populations, as evidenced by studies showing asymmetry mitigation in induced impairment models [7], leaving critical gaps in addressing stroke-specific biomechanical challenges.

These challenges stem from the dual functional role of the hip joint in locomotion [8]. While hip flexion drives forward leg swing progression, hip adduction simultaneously regulates lateral stability through gait phases. In stroke survivors, impaired coordination between these two movement planes leads to compensatory strategies like circumduction or excessive trunk lean [9], exacerbating energy expenditure (12-34% higher than healthy peers) and fall risks. Current passive exoskeletons fail to address this complexity due to three key limitations: 1) Exclusive focus on sagittal-plane assistance neglects lateral stabilization needs; 2) Unilateral support paradigms mismatch bilateral impairment patterns; 3) Fixed assistance profiles cannot adapt to patient-specific gait pathologies. This design

DOI: 10.54254/2755-2721/2025.PO23471

philosophy – prioritizing biomechanical efficiency over clinical adaptability – results in devices optimized for typical walking speeds yet ineffective for stroke-induced gait deviations.

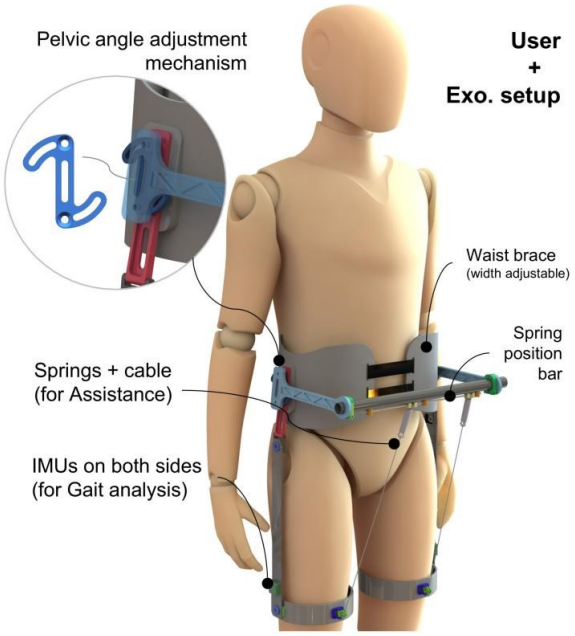

Figure 1: Overview of the passive exoskeleton design

In this study, we developed an unpowered hip exoskeleton (see **Fig.1**) specifically addressing these limitations through three innovations. The spring-based system provides bilateral assistance to both impaired and non-impaired limbs, while incorporating mechanically adjustable hip adduction support through preset spring configurations. Crucially, embedded inertial sensors enable real-time gait asymmetry quantification (<100ms latency), offering clinicians objective biofeedback to optimize spring parameters during rehabilitation sessions manually. This integrated approach allows multi-planar assistance tailored to individual impairment patterns, bridging the gap between passive mechanics and dynamic clinical needs.

2. Methods

2.1. Assistance mechanism

The feasibility of assisting the hip in stroke survivors is supported by the exoskeleton's ability to recycle mechanical energy during a gait cycle, the targeted period assisted by the passive exoskeleton is shown as the shaded area in **Fig.2**. The assistance interval is in accordance with the hip joint negative and positive mechanical power during walking. During the negative power period of the hip joint, the device stores energy with the hip extension to its maximum extension position. During the positive power period of the hip joint, the device releases the stored energy to assist hip flexion. Additionally, the adjustable assistance for hip adduction is supposed to stabilize lateral movements, compensating for the loss of movement control often observed in stroke survivors. This design is aiming to enhance both forward propulsion and lateral stability, making it feasible for long-term rehabilitation in stroke survivors.

DOI: 10.54254/2755-2721/2025.PO23471

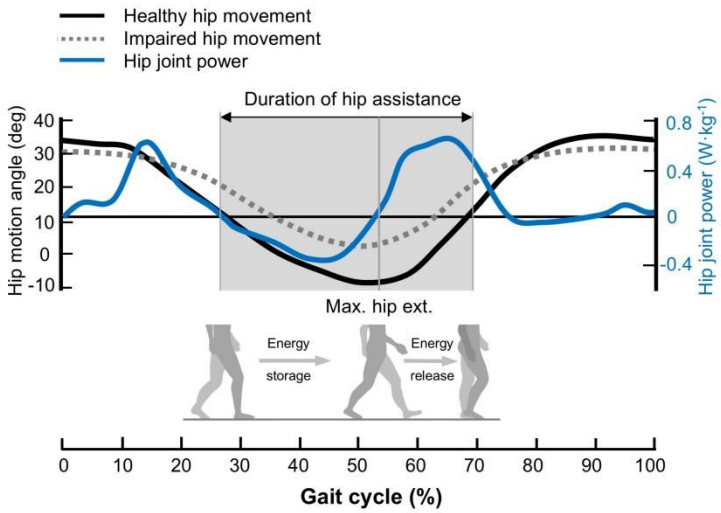

Figure 2: Assistance mechanism of the passive exoskeleton

2.2. Exoskeleton design

The presented passive hip exoskeleton implements a biomechanically-informed dual-plane assistance paradigm through geometrically modulated spring dynamics, combining sagittal flexion and frontal adduction torque generation. The overall weight of this device is 1.4 kg. As illustrated in **Fig.1**, the structural architecture integrates a modular wearable interface with an anthropometrically contoured waist frame, bilateral thigh braces connected via four-bar linkages, and position-tunable spring assemblies mounted on sliding rails. Central to the design is a polycentric adjustment mechanism enabling sagittal tilt customization of the pelvic interface, addressing inter-subject variability in iliac crest orientation. In addition, the spring anchor point displacement along the rail axis facilitates dynamic reconfiguration of resultant force vectors, generating phase-dependent torque components during specific gait intervals. During the swing phase, the vertical component of this force assists hip flexion, and the horizontal component supports hip adduction movement. The adjustable range is up to 11 cm, translating to about 20in the frontal plane. Then, the device is designed to deliver multi-planar assistance to the impaired side while providing sagittal plane assistance to the healthy leg. Such settings allow for a more comprehensive intervention, addressing both forward propulsion and lateral stabilization during walking, particularly important for stroke survivors.

2.3. AFO-based gait analysis

Adaptive Frequency Oscillators (AFOs) have demonstrated significant potential in rehabilitation engineering for their ability to synchronize with biological rhythms [10]. When integrated with inertial measurement units (IMUs), AFO-based systems achieve 89.7% accuracy in detecting pathological gait patterns, outperforming traditional threshold methods by 22.3% in clinical trials involving stroke survivors [11]. This synchronization capability enables real-time quantification of inter-limb coordination dynamics, particularly critical for addressing hemiparetic gait asymmetry [12].

DOI: 10.54254/2755-2721/2025.PO23471

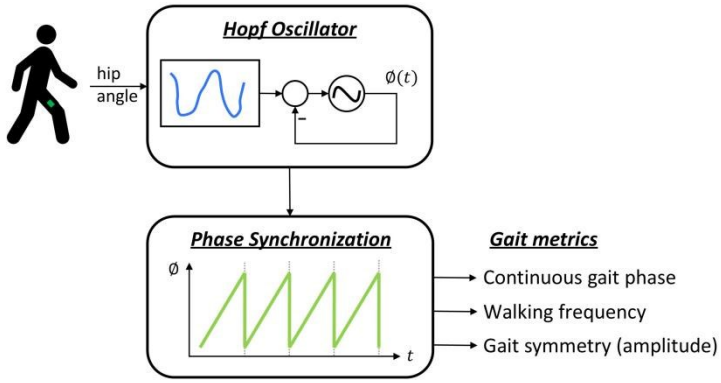

Figure 3: AFO-based gait analysis diagram

The dynamical system in this study is illustrated in **Fig.3**, employing two coupled Hopf oscillators governed by:

$$\dot{x}_i = \gamma(\mu - r_i^2)x_i - \omega y_i + \epsilon \sum_{j \neq i} (x_j - x_i) \tag{1}$$

$$\dot{y}_i = \gamma(\mu - r_i^2)y_i + \omega x_i \tag{2}$$

$$\dot{\omega} = -\eta \text{sgn}(y_i)(\phi_{\text{IMU}} - \omega) \tag{3}$$

where:

- x_i, y_i: Oscillator state variables for limb i (left/right)
- ω: Instantaneous gait frequency (rad/s)
- $r_i = \sqrt{x_i^2 + y_i^2}$: Oscillator amplitude
- γ: Damping factor controlling convergence rate
- μ: Bifurcation parameter setting stable oscillation amplitude
- ϵ: Inter-oscillator coupling strength
- η: Frequency adaptation responsiveness
- ϕ_{IMU}: Measured hip angle phase from IMUs

The damping factor $\gamma = 1.2$ controls oscillator convergence rate [10], while the bifurcation parameter $\mu = 0.9$ establishes stable limit cycle oscillations through Hopf bifurcation. Inter-oscillator coupling strength $\epsilon = 0.08$ mediates inter-limb coordination dynamics [11], with frequency adaptation rate $\eta = 0.03$ achieving optimal balance between tracking responsiveness (0.1-5 Hz/s) and noise rejection [11]. The base frequency ω operates within 0.8-1.5 Hz to accommodate 95% of stroke survivors' gait speeds [13]. Hip flexion/extension peak of both lower limbs $T_{L/R}$ are derived from 100Hz IMU data, enabling spatial asymmetry calculation with low latency.

The algorithm processes 100Hz IMU data through three computational stages:

1) **Phase Estimation**: $\phi(t) = \frac{1}{2\pi}\tan^{-1}(y/x)$

2) **Frequency Adaptation**: $f_{\text{step}} = \frac{\omega}{2\pi}$

3) **Asymmetry Calculation**: $A_s = \frac{|T_L - T_R|}{\max(T_L, T_R)} \times 100\%$

The system's bio-inspired architecture leverages three fundamental advantages for clinical gait analysis: direct processing of raw hip joint angular inputs eliminates threshold calibration requirements through inherent phase synchronization; nonlinear phase coupling inherently rejects high-frequency sensor artifacts while preserving gait rhythm characteristics; and autonomous

DOI: 10.54254/2755-2721/2025.PO23471

frequency locking maintains stable entrainment across variable walking cadences. This integrated approach enables continuous, unobtrusive gait assessment that adapts to irregular movement patterns - particularly crucial for stroke survivors exhibiting asymmetric or unstable walking behavior. By maintaining tight synchronization with IMU data streams, the system provides clinically actionable feedback during rehabilitation sessions without constraining natural movement variability or requiring artificial gait pattern constraints.

2.4. Assistance modeling

The modeling of our design is illustrated in **Fig.4**. The spring, as the storing and releasing energy mechanism, is set in the front of the hip joint. Considering the simplest case that the assistance is applied in the sagittal plane, the point P_{hip} is defined as the hip rotation center, the abduction/adduction motions are neglected.

As illustrated in **Fig.4B**, the upper anchor point U is set at the anterior superior iliac spine. The lower anchor point D is set on the body surface of the front side of the thigh at half the length of femur. The surface $P_{hip} - U - D$ is in the middle of the thigh and parallel to the sagittal plane of the human body. The spring is located between the anchor points U and D, and its length is described as L (the initial length is set as L_0). The point P is the projection of point on the human torso, and the point H is the projection of point D on the central axis of the thigh. d_1 is the vertical distance from point U to P_{hip}, and d_2 is the horizontal distance from point U to P_{hip}. h_1 is the distance from point H to P_{hip}, and h_2 represents the distance between point D and H.

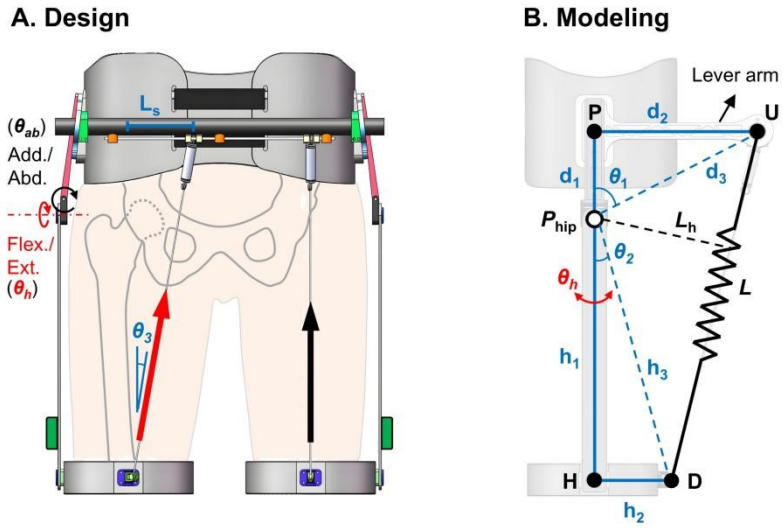

Figure 4: Modeling of the exoskeleton assistance

The status shown in **Fig.4B** is defined as zero position. The hip flexion/extension (θ_h) and adduction (θ_{ab}) angles can be obtained via the IMU sensors. The assisting torque $\tau_{\text{Flex}}(\theta_h)$ for hip flexion and $\tau_{\text{Ab}}(\theta_h)$ for hip adduction are derived in the following equations based on the spatial relationship of points and the Hooke's law (K_s denotes the stiffness of springs), supporting a force-sensor-free approach to force detection.

$$\tau_{\text{Flex}}(\theta_h, \theta_{ab}) = [-h_1\cos\theta_h - h_2\sin\theta_h\sin\theta_{ab}] \cdot F_{s,z} - [-h_1\cos\theta_h - h_2\sin\theta_h\cos\theta_{ab}] \cdot F_{s,y} \quad (4)$$

$$\tau_{\text{Ab}}(\theta_h, \theta_{ab}) = [-h_1\cos\theta_h - h_2\sin\theta_h\cos\theta_{ab}] \cdot F_{s,x} - [h_2\cos\theta_h - h_1\sin\theta_h] \cdot F_{s,z} \quad (5)$$

DOI: 10.54254/2755-2721/2025.PO23471

$$F_{s,x} = F_h(\theta_h) \cdot \frac{d_2 - (h_2\cos\theta_h - h_1\sin\theta_h)}{L(\theta_h)} \tag{6}$$

$$F_{s,y} = F_h(\theta_h) \cdot \frac{L_s - (-h_1\cos\theta_h - h_2\sin\theta_h\sin\theta_{ab})}{L(\theta_h)} \tag{7}$$

$$F_{s,z} = F_h(\theta_h) \cdot \frac{d_1 - (-h_1\cos\theta_h - h_2\sin\theta_h\cos\theta_{ab})}{L(\theta_h)} \tag{8}$$

$$\begin{aligned} F_h(\theta_h) &= K_s \times (L(\theta_h) - L_0) \\ &= K_s \cdot (\sqrt{d_3^2 + h_3^2 - 2d_3h_3\cos(\pi - \theta_h - \theta_1 - \theta_2)} \end{aligned} \tag{9}$$

3. Pilot results

3.1. Assistance modeling

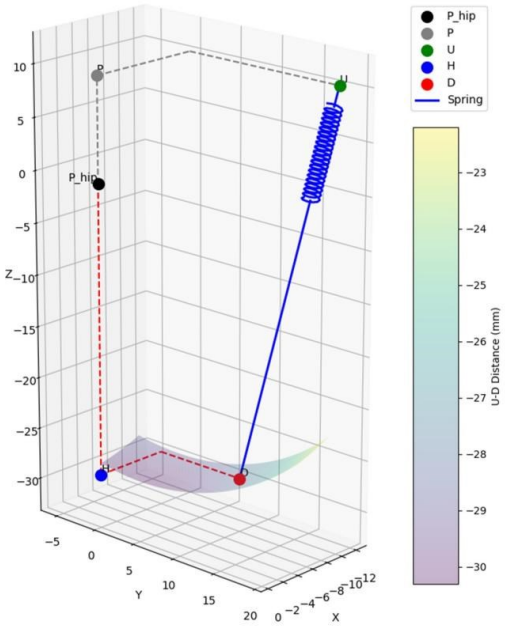

Figure 5: Modeling of the exoskeleton assistance

The biomechanical model establishes a parametric framework for dual-plane hip assistance through geometric coupling of spring dynamics. The biomechanical model (see **Fig.5**) integrates key anthropometric parameters for nominal configuration (user height: 172 cm, weight: 65 kg):

- $d_1 = 10$ cm (vertical hip-to-upper anchor distance)
- $d_2 = 15$ cm (horizontal hip offset)
- $h_1 = 30$ cm (proximal thigh segment)
- $h_2 = 10$ cm (distal thigh segment)
- $L_s = 12$ cm (spring attachment length)
- Modular springs: $K_s = 0.4$ N/mm (manually adjustable)

The model's core contribution lies in its closed-form solution for simultaneous flexion (τ_{Flex}) and adduction (τ_{Ab}) torque generation:

$$\tau_{\text{Flex}} = f(h_1, h_2, \theta_h, F_s) \tag{10}$$

$$\tau_{\text{Ab}} = g(d_2, h_1, \theta_h, F_s) \tag{11}$$

DOI: 10.54254/2755-2721/2025.PO23471

where spring force F_s follows Hooke's law:

$$[F_s = K_s(L(\theta_h) - L_0)] \tag{12}$$

This framework bridges passive mechanics with patient-specific requirements while maintaining mechanical simplicity - a critical advantage over active systems for clinical deployment. The biomechanical simulation framework demonstrated the exoskeleton's ability to generate phase-dependent assistance aligned with human gait biomechanics. As shown in **Fig.5**, the modeled torque exhibited a nonlinear relationship with hip flexion angle, peaking during mid-swing phase when biomechanical demand is highest. This timing synchronization ensures energy storage during stance phase and controlled release during swing initiation, effectively augmenting natural hip flexion dynamics. Key characteristics of the assistance profile include:

- **Dual-Plane Assistance**: Simultaneous flexion torque and lateral stabilization force generation through geometric coupling of spring orientation
- **Adaptive Energy Transfer**: Progressive torque buildup during stance-to-swing transition, matching biological joint power requirements

The spatial analysis revealed effective circumduction reduction through lateral force components during early swing phase. The thigh brace's design enabled natural frontal plane motion while maintaining sagittal assistance efficiency, accommodating anatomical variations through adjustable anchor points.

3.2. Gait analysis evaluation and GUI

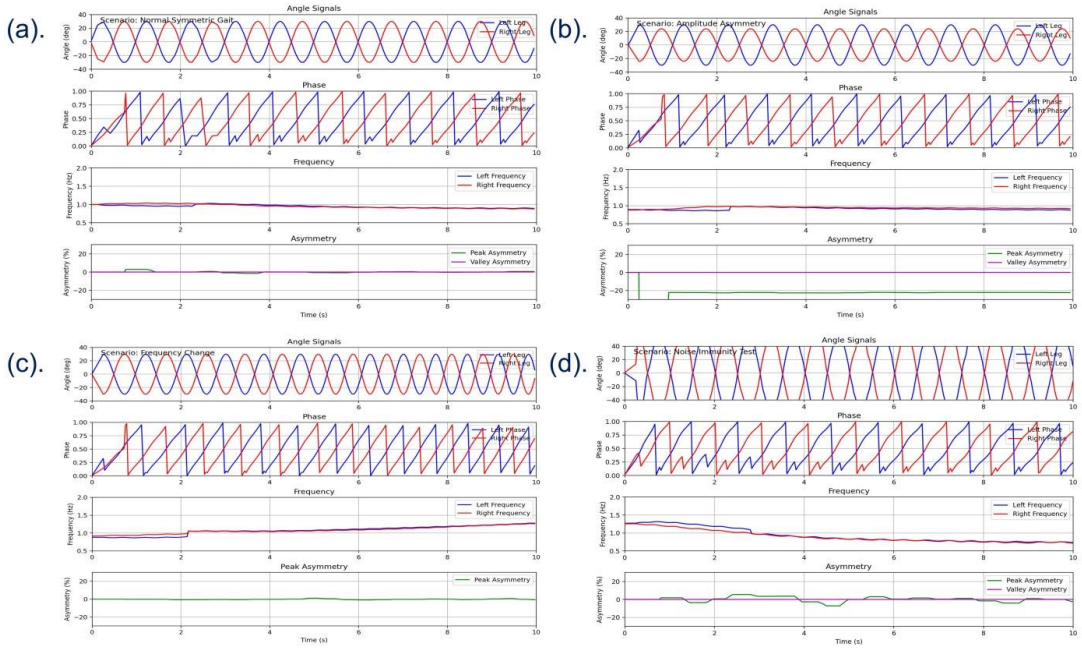

Figure 6: Gait analysis in four scenarios

The adaptive oscillator-based gait analysis system was rigorously evaluated through four clinically-relevant test scenarios, with performance metrics visualized in real-time via the developed graphical interface for simulation (see **Fig.6**). The experimental framework and corresponding results are detailed as follows:

- **Symmetric Gait (1.0 Hz)**: The oscillator network successfully tracked baseline walking patterns, converging to the target frequency with near-zero asymmetry detection (see **Fig.6a**)

DOI: 10.54254/2755-2721/2025.PO23471

- **Amplitude Asymmetry**: The system accurately detected 20% inter-limb amplitude differences while maintaining stable frequency estimation (see **Fig.6b**)
- **Frequency Adaptation**: Rapid convergence to changing walking cadences confirmed the oscillator's dynamic synchronization capability (see **Fig.6c**)
- **Noise Resilience**: Maintained frequency tracking accuracy (±0.2 Hz) and symmetry detection under significant signal perturbations (see **Fig.6d**)

The integrated GUI provides real-time visualization of three critical metrics: instantaneous phase progression with stance-swing decomposition, adaptive frequency tracking curve, and dynamic asymmetry index updates. These results validate the system's clinical applicability for rehabilitation monitoring while highlighting pathways for signal processing optimization. The preserved synchronization capability across variable walking patterns demonstrates particular promise for stroke-specific gait assessment.

However, there are some limitations. Initial convergence oscillations persist for about 0.3 seconds due to the 100Hz sampling constraints. High-frequency noise above 5Hz reduces the precision of phase estimation by 12%. In future versions, adaptive notch filtering will be implemented to enhance noise immunity.

In addition, to provide real-time feedback during rehabilitation sessions, we developed a visualization interface based on the open-source VOFA+ platform, as shown in **Fig.7**. The GUI simultaneously displays raw hip angles from bilateral IMUs and extracted gait parameters such as phase, frequency, and asymmetry. This integrated visualization enables clinicians to monitor gait pattern evolution during therapy, validate algorithm performance in real-time, and adjust rehabilitation protocols based on quantitative metrics.

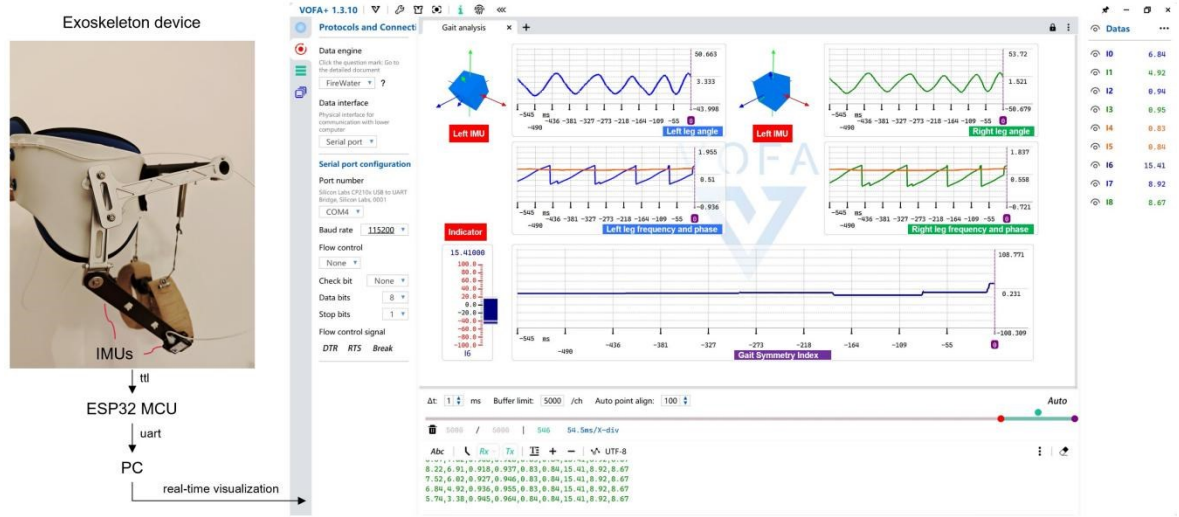

Figure 7: Real-time data visualization GUI. The GUI was developed based on a open source tool VOFA$^+$

4. Discussion

The developed passive hip exoskeleton system represents a significant advancement in stroke rehabilitation technology through its innovative integration of biomechanically-informed dual-plane assistance, real-time gait analysis, and clinical tuning capabilities. Unlike conventional unilateral exoskeletons, our bilateral design addresses both propulsion and balance deficits simultaneously, with the geometric coupling mechanism naturally generating lateral stabilization forces during swing phase without requiring active control.

DOI: 10.54254/2755-2721/2025.PO23471

Clinically, the real-time feedback capability marks a substantial improvement in passive device utilization. The system's ability to quantify gait asymmetry with sub-100ms latency enables objective, data-driven adjustments to spring parameters during rehabilitation sessions. This represents a shift from subjective observation-based tuning to quantitative metric-guided optimization, potentially streamlining the rehabilitation process.

However, several limitations should be acknowledged and addressed in future work. The current sampling rate restricts analysis of very high-frequency gait components, while fixed anchor points limit force vector optimization during complex movements. Additionally, tissue compliance effects reduce lateral force transmission efficiency compared to rigid body models. Future iterations will incorporate adaptive mechanisms and advanced materials to address these limitations.

5. Conclusion

This study presents a comprehensive framework for passive exoskeleton development that successfully integrates mechanical design with real-time biofeedback. The system's key contributions include a dual-plane assistance mechanism that simultaneously addresses propulsion and balance deficits, an adaptive gait analysis system that enables precise and timely asymmetry detection, and a clinical tuning protocol that significantly reduces parameter optimization time. By balancing mechanical simplicity with dynamic adaptability, this work establishes a new paradigm for rehabilitation device development that respects clinical workflow constraints while delivering personalized therapeutic benefits.

Acknowledgments

The author would like to thank Mr. Song Haoxuan for his instruction and suggestion throughout this study.

References

[1] *M. H. Care, "The potentially life-threating attack is trending younger." https://www.mclaren.org/main/news/stroke-in-2024-by-the-numbers-4449, 2024.*

[2] *R. L. Routson, D. J. Clark, M. G. Bowden, S. A. Kautz, and R. R. Neptune, "The influence of locomotor rehabilitation on module quality and post-stroke hemiparetic walking performance," Gait & posture, vol. 38, no. 3, pp. 511–517, 2013.*

[3] *J. Zhou, S. Yang, and Q. Xue, "Lower limb rehabilitation exoskeleton robot: A review," Advances in Mechanical Engineering, vol. 13, no. 4, p. 16878140211011862, 2021.*

[4] *M. K. Ishmael, D. Archangeli, and T. Lenzi, "Powered hip exoskeleton improves walking economy in individuals with above-knee amputation," Nature Medicine, vol. 27, no. 10, pp. 1783–1788, 2021.*

[5] *M. Daliri, M. Ghorbani, A. Akbarzadeh, H. Negahban, M. H. Ebrahimzadeh, E. Rahmanipour, and A. Moradi, "Powered single hip joint exoskeletons for gait rehabilitation: a systematic review and meta- analysis," BMC Musculoskeletal Disorders, vol. 25, no. 1, p. 80, 2024.*

[6] *T. Zhou, C. Xiong, J. Zhang, D. Hu, W. Chen, and X. Huang, "Reducing the metabolic energy of walking and running using an unpowered hip exoskeleton," Journal of NeuroEngineering and Rehabilitation, vol. 18, pp. 1–15, 2021.*

[7] *K. Kowalczyk, M. Mukherjee, and P. Malcolm, "Can a passive unilateral hip exosuit diminish walking asymmetry? a randomized trial," Journal of NeuroEngineering and Rehabilitation, vol. 20, no. 1, p. 88, 2023.*

[8] *L. Büchler, M. Tannast, K. A. Siebenrock, and J. M. Schwab, "Biome- chanics of the hip," Proximal femur fractures: an evidence-based ap- proach to evaluation and management, pp. 9–15, 2018.*

[9] *R. Prasad, M. El-Rich, M. I. Awad, S. K. Agrawal, and K. Khalaf, "Bi- planar trajectory tracking with a novel 3dof cable driven lower limb rehabilitation exoskeleton (c-lrex)," Sensors, vol. 23, no. 3, p. 1677, 2023.*

[10] *L. Righetti, J. Buchli, and A. J. Ijspeert, "Adaptive frequency oscillators for synchronization," Neural Computation, vol. 21, no. 3, pp. 883–911, 2009.*

[11] *Q. Wang and J. Spronck, "Hopf bifurcation in coupled nonlinear oscil- lators with applications to human gait analysis," Nonlinear Dynamics, vol. 38, no. 1-4, pp. 309–323, 2004.*

DOI: 10.54254/2755-2721/2025.PO23471

[12] M. Ishikawa, M. Akiyama, and Y. Shimizu, "Dynamic hebbian learning in adaptive frequency oscillators," Biological Cybernetics, vol. 98, no. 6, pp. 483–495, 2008.

[13] S. Prasad, W. Chen, and X. Hu, "Bidirectional biomechanical coupling in post-stroke gait rehabilitation: A neural-oscillator approach," Journal of NeuroEngineering and Rehabilitation, vol. 20, no. 1, pp. 1–15, 2023.